et al., Phys. Rev. Letters 23, 528 (1969).
[5]Overlap singularities: see, for example, S. Doniach and M. Sunjic, J. Phys. C 3, 284 (1970).
[6]S. Doniach, Phys. Rev. B (to be published).
[7]J. Gavoret, P. Nozières, B. Roulet, and M. Combescot, J. Phys. (Paris) 30, 987 (1969).
[8]E. P. Gross, in *Mathematical Methods in Solid State and Superfluid Theory* (Oliver and Boyd, Edinburgh, 1967), p. 46.
[9]R. Kubo, J. Phys. Soc. Japan 17, 1100 (1962).
[10]R. M. Wilcox, J. Math. Phys. 8, 962 (1967).
[11]K. D. Schotte and U. Schotte, Phys. Rev. 182, 479 (1969).
[12]S. Tomonaga, Progr. Theoret. Phys. (Kyoto) 5, 544 (1950).
[13]P. W. Anderson, Phys. Rev. Letters 18, 1049 (1967).
[14]See D. R. Hamann, Phys. Rev. B 2, 1373 (1970).
[15]N. I. Muskhelishvili, *Singular Integral Equations* (P. Noordhoff, Ltd., Groningen, The Netherlands, 1953), Chap. 14.
[16]See, for instance, P. Nozières, *Interacting Fermi Systems* (Benjamin, New York, 1964), Chap. 5.
[17]See, for example, W. E. Spicer, Phys. Rev. 154, 385 (1967) and references therein for an account of photoemission experiments.
[18]See, for example, *Polarons and Excitons* (Oliver and Boyd, Edinburgh, 1962).
[19]K. D. Schotte and U. Schotte, Phys. Rev. 185, 509 (1969).
[20]See, for example, *Hyperfine Structure and Nuclear Radiation*, edited by E. Matthias and D. A. Shirley (North-Holland, Amsterdam, 1968).
[21]J. J. Hopfield, Commun. Solid State Phys. 11, 40 (1969).
[22]S. S. Schweber, *An Introduction to Relativistic Quantum Field Theory* (Harper and Row, New York, 1961), Chap. 12.
[23]D. R. Yennie, in *Lectures on Strong and Electromagnetic Interactions*, edited by K. W. Ford (Brandeis Lecture Notes, Boston, 1964), p. 165.
[24]N. Rosen and C. Zener, Phys. Rev. 40, 502 (1932).

PHYSICAL REVIEW B VOLUME 3, NUMBER 4 15 FEBRUARY 1971

Lattice Thermal Conductivity of Plastically Deformed Copper plus 10 Atomic Percent Aluminum Specimens in the Temperature Range 1–4 °K*

M. A. Mitchell,† P. G. Klemens, and C. A. Reynolds
Physics Department and Institute of Materials Science, University of Connecticut, Storrs, Connecticut 06268
(Received 5 June 1970)

The total thermal and electrical conductivities of seven polycrystalline rods of copper plus 10 at.% aluminum, which were in a total of 25 different states of recovery from plastic deformation at 77 °K, and one commercially pure nickel single crystal were measured in the liquid-helium temperature range. The low-temperature lattice thermal conductivity of a specimen which had been plastically deformed 9% recovered slowly as it was annealed between 300 and 700 °K, and then rapidly recovered to its prestrain magnitude after being annealed between 700 and 800 °K. The recrystallization temperature was 725 °K. Metallographic grain-size studies supported these conclusions. An application of the theory of Klemens and Ackerman and Klemens to the variation of the dislocation lattice thermal resistivity with annealing temperature (below 700 °K) due to impurity atmospheres made it possible to determine the fractional atomic-volume difference α between the aluminum and copper atoms to be 0.23. When the same theory was compared with variation of the dislocation lattice thermal resistivity with aluminum concentration found by Charsley, Salter, and Leaver, it was found that $\alpha = 0.24$. From the experimental x-ray data, α is 0.20. A later theory of Klemens which treated the variation of dislocation resistivity with annealing time at fixed annealing temperature was found to be inconsistent with the data of this work, but the experimental error was large. The theory contained the assumption that a unique diffusion constant could be defined for the deformed alloys, but this may not have been true, since plastic deformation generates excess vacancies. An anomalous departure of the phonon-electron lattice thermal resistivity from a T^{-2} temperature dependence was thought to be an effect associated with the small electron mean free paths in these alloys. The theory of Lindenfeld and Pennebaker qualitatively explained the anomaly.

I. INTRODUCTION

The lattice conductivity of a metal is sensitive to defects in the crystal structure. The different types of defect give rise to lattice thermal resistivities[1] which have their own characteristic temperature dependences. Plastic deformation generates dislocations; these produce a lattice thermal resistivity which is proportional to T^{-2}. Charsley *et al.*[2] found that the thermal resistivity per dislocation had a concentration dependence in copper-aluminum alloys which could not be explained by the

then-existing theory.[1] Klemens[3] suggested a model in which impurities modulate the strain field of the dislocations to explain the concentration dependence of the thermal resistivity (this will be discussed in detail in Sec. IV). It is the purpose of this work to investigate the variation of dislocation thermal resistivity with annealing time and temperature, and test the predictions of the theory of Klemens,[3,4] and Ackerman and Klemens.[5]

The total thermal flux in a metal is the sum of the fluxes carried independently by the conduction electrons and the lattice. The total thermal conductivity K is thus the sum of electronic thermal conductivity K_e and the lattice thermal conductivity K_g (e.g., see Ref. 6):

$$K = K_e + K_g \quad . \tag{1}$$

In this copper-aluminum alloy, the electrical resistivity ρ_0 is constant in the liquid-helium temperature range, and is due to elastic scattering of electrons by point defects and lattice defects.

At low temperatures in a concentrated alloy, the electronic conductivity is related to the residual resistivity through the Wiedemann-Franz law (e.g., see Ref. 6):

$$K_e = L_0 T/\rho_0 \quad , \tag{2}$$

where L_0 and T are the ideal Lorenz number (2.445×10^{-8} WΩK^{-2}) and the absolute temperature, respectively.

The lattice conductivity may be found by subtracting K_e of Eq. (2) from the total thermal conductivity,

$$K_g = K - L_0 T/\rho_0 \quad . \tag{3}$$

The lattice conductivity was found in this way for the specimens considered in this investigation.

The lattice conductivity is sensitive to lattice defects, and in particular, each type of defect will give rise to a characteristic temperature dependence. In order to study the effect of each defect on the lattice conductivity, use is made of the additive-resistance approximation (see Klemens[7] for a discussion of the use and validity of the approximation)

$$W_g = 1/K_g = \sum_i W_i \quad , \tag{4}$$

where W_g is the total lattice thermal resistivity, and W_i is the lattice thermal resistivity due to the ith type of defect.

In a well-annealed alloy, the lattice thermal resistivity is due to scattering of phonons by electrons in the temperature range 1–4 °K. According to early theories, the temperature variation of the phonon-electron thermal resistivity W_{pe} is T^{-2}. Experimentally there were deviations from T^{-2} which will be discussed in detail in Sec. IV. Lattice thermal resistivity due to point defects is not important at these low temperatures. Klemens[1] discusses these and other lattice thermal resistivities, and their characteristic temperature dependences.

The specimens of this investigation were tensilely and torsionally deformed in the plastic-flow region up to about 9% (except one specimen which was swaged from a relatively large diameter, and thus cold-worked several hundred percent), and thus dislocations were generated in large numbers.

Cottrell[8] gives a review of the theory of dislocations in terms of elastic continuum theory. Dislocations scatter phonons in the liquid-helium temperature range. Thus the total lattice thermal resistivity of these copper-aluminum specimens will arise from scattering of phonons by both electrons and dislocations; individual point defects produce no significant scattering in this temperature range and other defects are probably negligible also. The lattice dislocation thermal resistivity W_{gd} has been the subject of a number of previous studies, among which were Kemp *et al.*,[9] Lomer and Rosenberg,[10] and Kemp *et al.*[11] which showed that the theory correctly predicted the observed T^{-2} temperature dependence of W_{gd}. These studies were also concerned with correlating the dislocation density N_d estimated from the theoretical expression[1] for dislocation thermal resistivity with the dislocation density found by experimental stored-energy measurements,[12] and direct observation with an electron microscope.[10] The thermal estimates yielded N_d's, which were a factor of about six higher than the experimental estimates. This discrepancy was not explained theoretically.

In Sec. II of this paper, the preparation and condition of the specimens will be discussed. Section III is a brief discussion of the experimental techniques used. Section IV is a short outline of the modified Klemens theory. In Sec. V the experimental data will be presented. Sec. VI will summarize the results and conclusions.

II. SAMPLE PREPARATION

The copper plus 10 at.% aluminum specimens were obtained from the Materials Research Corp. (Orangeburg, N. Y.). The alloy was prepared by vacuum induction melting 4.5% by weight of 99.999% pure aluminum with 99.999% pure copper. The resulting slug was machined to remove the surface contamination and slag, and then swaged (from about 1 in. diam) without annealing to a $\frac{3}{16}$ in. diam.

Half of the $\frac{3}{16}$ in. stock was swaged to a $\frac{1}{8}$ in. diam. The $\frac{1}{8}$ in. stock was put into liquid nitrogen and kept there until a section designated sample A was cut off and mounted (at 273 °K) for the thermal conductivity measurement; it was in a very heavily

cold-worked condition. The diameters were found to be within 0.0002 in. of their nominal values.

A nickel single crystal was measured and used to test the apparatus and thermometer calibration. This sample (99.9% pure with Fe, Si, and C impurities) was grown from a seed crystal in an alumina crucible using a variation of the Bridgman method. A ⟨111⟩ axis was oriented along the sample axis. Annealing was carried out at 930 °C for 48 h in a quartz tube sealed off under vacuum.

III. EXPERIMENTAL DETAILS

The thermal conductivity was measured by previously described techniques,[13] with the following exceptions: An apparatus similar to the one in Fig. 1(b) of Ref. 13 was used to measure samples A, B, and $C1$–$C4$ (all of these were $\frac{1}{8}$ in. diam before plastic deformation), i.e., the samples extended through the can top into the bath. The remaining specimens ($\frac{3}{16}$ in. diam before plastic deformation) were mounted in good thermal contact to a pure-copper post, which in turn extended through the can top into the bath; this method resulted in lower temperature differences between the thermometers at zero heater power. The vacuum space of the adiabatic can surrounding the specimens was monitored periodically with a Veeco MS-90A leak detector, both above and below the λ point, to be sure that there were no leaks.

The two germanium resistance thermometers were calibrated against the vapor pressure of the liquid helium by submerging them (surrounded only by a radiation shield) in the liquid helium inside a partially silvered glass Dewar. A bath-height correction was made to the surface pressure, which was measured by means of a mercury or Octoil-S manometer, whose manometer fluid-height difference was measured with a cathetometer. The vapor pressure was controlled by means of a Walker-type regulator.[14] Vapor pressures were reduced to absolute temperatures T using the 1958 Liquid-Helium Vapor-Pressure Tables.[15] Thermometer current and potential measurements were made using previously described electronics.[16]

About 20 sets of resistance R and temperature T calibration points were thus obtained in the temperature range 1–4 °K for each thermometer. A least-squares fit of each of these sets was made to the equation

$$T_R(R_i)=\left(A+\frac{B}{\ln R_i}+C\ln R_i+\frac{D}{(\ln R_i)^2}+E(\ln R_i)^2\right)^{-1} .$$

A deviation curve drawn through the points $T_R(R_i) - T_i$ plotted against $T_R(R_i)$, was used to make small corrections to $T_R(R_i)$ for each thermometer. It was necessary to smooth relatively large (≈ 0.013 °K) deviations in the temperature range 2.2–2.6 °K to reduce scatter in the K/T vs T data.

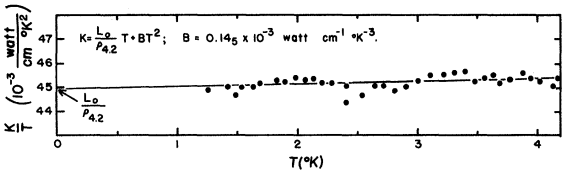

FIG. 1. Ratio of total thermal conductivity K to absolute temperature T is plotted against T for a commercially pure- (99.9%) nickel specimen. Solid line is a straight line drawn through the experimental data; it intercepts the axis at L_0/ρ_0. Thus, total thermal conductivity is the sum of the electronic (L_0T/ρ_0) and a small lattice (BT^2) thermal conductivity. Note that there is no kink. These results are considered to be an adequate verification of the measurement technique.

Figure 1 shows the final results for the nickel specimen. According to Erdmann and Jahoda,[17] the total thermal conductivity should follow the equation

$$K=L_0T/\rho_0+BT^2 , \qquad (5)$$

where BT^2 is the lattice thermal conductivity. As can be seen from Fig. 1, the data points all lie close to a line predicted by Eq. (5). The fact that the present value of B agrees within 10% with that of Erdmann and Jahoda gives us confidence in our procedures. The temperature measurement was thought to be accurate to less than 0.001 °K judging from the internal consistency of the data.

Temperature differences with the heater power on were maintained between 0.130 and 0.550 °K over a distance of 7 cm. The data taken with different heater power settings were self-consistent. Temperature differences of the order of ±0.001 °K with the heater power off were noted, and these were subtracted algebraically from the power-on temperature differences, which resulted in less scatter.

A 1% correction was made for the joule heat generated in the manganin heater leads. No other corrections were greater than 0.1%, and were therefore neglected. The probable error[18] in total thermal conductivity was 0.5%; the probable error in lattice conductivity was 2–3%.

The electrical resistivity of the specimens was measured between the thermometer clamps so that the geometry factor was the same for both the thermal and electrical conductivity measurements. The techniques used were the same as those described previously by Gueths *et al.*,[19] and the propable error of the electrical resistivity was 0.2%.

In order to ensure that no inhomogeneities of the impurity or dislocation distributions of the specimens affected the measurements, a jig was constructed which allowed the thermometer mounts to be removed and replaced at definite fixed positions on the specimens. This maintained a separation of 7.00±0.02 cm between the thermometer clamps,

with the warm thermometer 4.06 cm from the heater end of the specimen. Thermometer mounts were made from No. 20 B & S gauge pure-copper wire which was held pressed against the sample by means of small screws.

IV. THEORY OF LATTICE THERMAL RESISTIVITY

Theory of Phonon-Electron Thermal Resistivity

A calculation of the lattice thermal resistivity due to scattering of phonons by electrons was made by Makinson[20] in 1938,

$$W_{pe}T^2 = 1/B_{pe} \quad . \tag{6}$$

The temperature dependence has been experimentally verified for a large number of different alloys, but Makinson's estimate of the constant B_{pe} was too high. Klemens[21] used a value of the phonon-electron interaction energy estimated from low-temperature ideal electronic thermal conductivity data to calculate

$$B_{pe}^{-1} = 720 \text{ cm } ^\circ\text{K}^3/\text{W}$$

for pure copper. This was in good agreement with the experimental results. This theory does not predict a concentration dependence of W_{pe} which has been experimentally observed in most alloys.

Makinson's calculation depends on assuming that the adiabatic principle holds for the conduction electrons and then applying second-order time-dependent perturbation theory to calculate the phonon mean free path. However, a criterion for the validity of this approach (see Sec. 5.12, Ref. 6) may be

$$q\,\Lambda_e > 1 \quad , \tag{7}$$

where q and Λ_e are the phonon wave number and the electron mean free path, respectively. For copper plus 10 at.% aluminum, $q\Lambda_e \approx 1$ at 4 °K, and the product grows smaller with decreasing temperature.

Pippard[22] derived an expression for the phonon mean free path for phonon-electron scattering which did not depend on the validity of Eq. (7). Lindenfeld and Pennebaker[23] used the Pippard expression to calculate the thermal conductivity for phonon-electron scattering, which showed that $W_{pe} \propto T^{-n}$, where n is a function of temperature. At low temperatures and relatively high residual resistivities $n \approx 1$, while at high temperatures $n \gtrsim 2$.

Theory of Dislocation Thermal Resistivity

Klemens[24] calculated the dislocation lattice thermal resistivity W_{gd}. His result was

$$W_{gd}T^2 = C\gamma^2 N_d \quad , \tag{8}$$

where γ and N_d are the Grueneisen constant and the dislocation density, respectively. The constant C was calculated theoretically.[25] It has to be increased[9] by a factor of 6 if it is to be brought into agreement with experimental work which correlated the dislocation densities estimated from Eq. (8) with densities derived from experimental stored-energy measurements[12] and electron-microscopic counts.[10] With this empirical correction we have

$$C = 0.75 \times 10^{-8} \text{ cm}^3 \ ^\circ\text{K}^3/\text{W} \quad .$$

Equation (8) was derived under the assumption that the dilatation Δ changes the frequency of a phonon of fixed wave vector, so that

$$\omega = \omega_0(1 - \gamma\Delta) \quad , \tag{9}$$

where ω_0 is the original frequency. The coefficient γ is the Grueneisen constant. However, impurities interact with dislocations and the impurity distribution c can be changed from its average value c_0 by the strain field of the dislocation. A difference in atomic mass between the host and impurity atoms can also produce a change in ω_0 which is proportional to $\beta(c - c_0)$, where

$$\beta = (M - M')/2M \quad , \tag{10}$$

and where M and M' are the atomic masses of the host and impurity, respectively.[10] If the atomic volume v of the impurity is different from the atomic volume of the host v_0 there will be a dilatation[5]

$$\alpha = (v - v_0)/v_0 \tag{11}$$

about an impurity, and a corresponding change $-\gamma\alpha(c - c_0)$ in ω_0. Thus, if these two effects are added to Eq. (9),

$$\omega = \omega_0[1 - \gamma\Delta + \beta(c - c_0) - \alpha\gamma(c - c_0)] \quad . \tag{12}$$

Cottrell[8] gives

$$c = c_0\, e^{-U_I/k_B T_a} \quad ,$$

where k_B and T_a are the Boltzmann constant and the annealing temperature at which the distribution was last at equilibrium, respectively. Cottrell[8] shows that the elastic interaction energy U_I of an impurity in the strain field of a dislocation is

$$U_I = -\alpha v_0 B \Delta \quad ,$$

where B is the bulk modulus. For $U_I/k_B T_a < 1$, one can approximate

$$c \simeq c_0(1 - U_I/k_B T_a) = c_0(1 + \alpha v_0 B\Delta/k_B T_a) \quad . \tag{13}$$

Since $W_{gd} \propto (\omega - \omega_0)^2$, one can write it in the form

$$W_{gd}T^2 = CN_d(\gamma + \gamma')^2 \quad , \tag{14}$$

where Eq. (13) has been substituted into Eq. (12), and

$$\gamma' \equiv (\alpha v_0 B/k_B T_a)\, c_0(\alpha\gamma - \beta) \quad . \tag{15}$$

Thus the impurity atmospheres lead to enhanced scattering if γ' is positive, and this enhancement depends on T_a, the temperature at which the atmospheres obtained equilibrium. This makes it possible to change the dislocation resistivity by anneal-

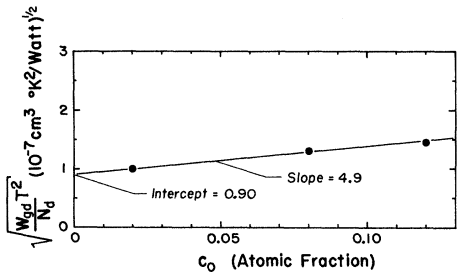

FIG. 2. According to the theory of Ackerman and Klemens the quantity $(W_{gd}T^2/N_d)^{1/2}$ is a linear function of c_0. W_{gd}, T, N_d, and c_0 are lattice dislocation thermal resistivity, absolute temperature, dislocation density, and atomic fraction of impurity, respectively. The three points are the experimental copper-aluminum data of Charsley *et al.* (Ref. 2). Solid straight line is drawn through the data points, and its slope and intercept are used to calculate the atomic volume of aluminum in copper.

ing.

These changes are, of course, not instantaneous, but are controlled by diffusion. Klemens[4] considered the time variation of W_{gd}:

$$W_{gd}T^2 = CN_d\{\gamma + \gamma'(T_{a2})[1 - (1 - T_{a2}/T_{a1})e^{-t_a/\tau_0}]\}^2 \ , \tag{16}$$

where t_a is the annealing time, T_{a1} is the annealing temperature at which the impurity distribution is at equilibrium at $t_a = 0$, and T_{a2} is the fixed annealing temperature for $t_a > 0$. Also, we have

$$1/\tau_0 = 9(6\pi^2)^{2/3}(T/\Theta)^2 D(T_{a2})/a^2 \ , \tag{17}$$

where T, Θ, a^3, and $D(T_{a2})$ are the measuring temperature, the Debye temperature, the atomic volume, and the diffusion constant at T_{a2} for the impurity in the host, respectively.

Charsley *et al.*[2] have experimentally measured $W_{gd}T^2/N_d$ as a function of aluminum concentration in copper. This dependence is not inconsistent with the above model. Equation (14) may be rewritten in the form

$$(W_{gd}T^2/N_d)^{1/2} = P + Q c_0 \ , \tag{18}$$

where

TABLE I. Sample history, residual resistivity, and annealing data.

Sample number	ρ_0 ($\mu\Omega$cm)	T_a (°K)	Time in oven (h)	Sample history
A	7.995	293 ± 60	3	As received from Materials Research Corporation (MRC).
B	7.461	1193 ± 50	48	MRC material was measured after anneal at left.
C1	7.468	300 ± 20	12	MRC material was annealed
*C*2	7.450	373 ± 1	48	1123 ± 70 °K for 28 h, then
*C*3	7.463	693 ± 50	20	given 9.5% torsional strain at
*C*4	7.404	713 ± 50	48	293 °K. It was reannealed (see left) before each set of measurements.
D	7.350	1205 ± 5	48	MRC material was measured after anneal at left.
*E*1	7.586	300 ± 40	12	MRC material was annealed at
*E*2	7.475	422 ± 5	48	1205 ± 5 °K for 48 h, then
*E*3	7.498	552 ± 13	48	given 9.33% tensile strain at
*E*4	7.542	673 ± 8	48	77 °K; maximum stress, 28.5
*E*5	7.456	797 ± 17	48	kg/mm^2; strain rate, 0.0093
*E*6	7.453	920 ± 6	48	sec^{-1}. Was reannealed (see
*E*7	7.441	1202 ± 5	48	left) before each set of measurements.
*F*1	7.567	360 ± 6	48	MRC material was annealed at
*F*2	7.536	564 ± 6	0.5	1202 ± 5 °K for 48 h, then given
*F*3	7.536	565 ± 8	1.5	8.13% tensile strain at 77 °K;
*F*4	7.498	567 ± 9	48	maximum stress, 29 kg/mm^2;strain
*F*5	7.498	570 ± 12	97	rate, 0.0081 sec^{-1}. Was reannealed (see left) before each set of measurements.
*G*1	7.644	344 ± 9	48	MRC material was annealed
*G*2	7.625	670 ± 15	0.5	1202 ± 5 °K for 48 h, then given
*G*3	7.612	661 ± 9	1.5	9.26% tensile strain at 77 °K;
*G*4	7.601	660 ± 6	48	maximum stress, 25.1 kg/mm^2; strain
*G*5	7.553	732 ± 6	48	rate, 0.004 sec^{-1}. Was reannealed (see left)
*G*6	7.576	1308 ± 20	48	before each set of measurements.
H	0.544	1200 ± 20	48	Nickel single crystal was measured after anneal at left.

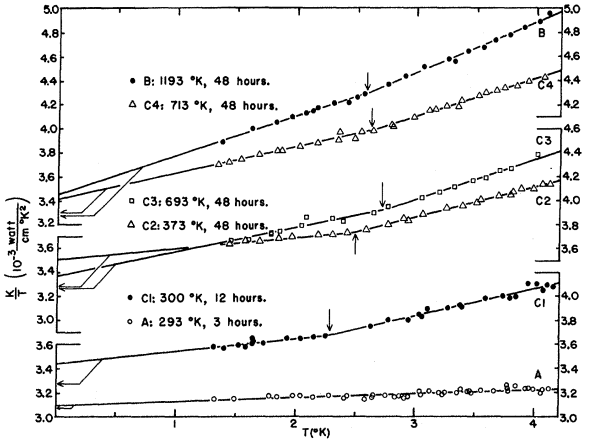

FIG. 3. Ratio of experimental total thermal conductivity K to absolute temperature T is plotted against T for specimens A, B, and $C1-C4$. Horizontal arrows indicate the ratio L_0/ρ_0, where L_0 and ρ_0 are the ideal Lorenz number and the residual resistivity, respectively. Solid straight lines through the data were fit by the method of least squares. There is a change in slope at the temperature indicated by the small vertical arrows. Annealing temperature and time in oven are indicated on the graph. Note that the heavily cold-worked specimen A has no perceptible change in slope.

$$Q/P=(1/\gamma)(\gamma\alpha^2-\beta\alpha)(v_0B/k_B T_a)\ . \qquad (19)$$

Rosenberg[26] cites experimental work in which it was determined that $\gamma\approx 1.8$ at low temperatures. Furthermore, we have $v_0B/k_B\approx 8.4\times10^4$ °K, $T_a\approx 300$ °K, and $\beta\approx 0.29$. If the theory is consistent with the data of Charsley *et al.*, according to Eq. (18) a plot

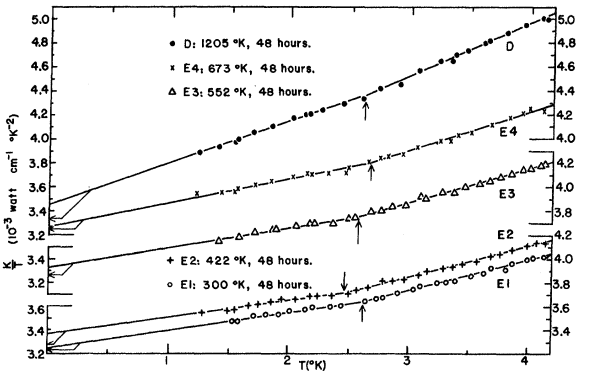

FIG. 4. Ratio of the experimental thermal conductivity K to the absolute temperature T is plotted against T for specimens D and $E1-E4$. Horizontal arrows indicate the ratio L_0/ρ_0, where L_0 and ρ_0 are the ideal Lorenz number and the residual resistivity, respectively. Solid straight lines through the data were fit by the method of least squares. There is a change in slope at the temperature indicated by the small vertical arrows. Annealing temperature and time in oven are indicated on the graph.

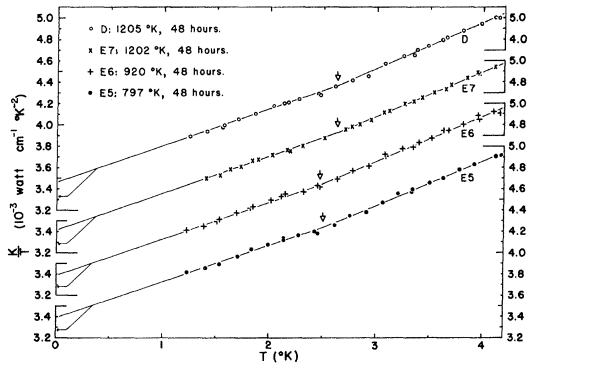

FIG. 5. Ratio of the experimental total thermal conductivity K to absolute temperature T is plotted against T for specimens D and $E5-E7$. Horizontal arrows indicate the ratio L_0/ρ_0, where L_0 and ρ_0 are the ideal Lorenz number and the residual resistivity, respectively. Solid straight lines through the data were fit by the method of least squares. There is a change in slope at the temperature indicated by the small vertical arrows. Annealing temperature and time in oven are indicated on the graph.

of $(W_{gd}T^2/N_d)^{1/2}$ vs c_0 should be linear. Figure 2 shows that it is. The ratio of the slope Q to the intercept P is 5.5. Solving Eq. (19) for α, one finds that $\alpha=0.24$. From the x-ray experimental results of the change of lattice spacing with aluminum concentration in copper, the atomic diameter of aluminum is 2.71 Å and of copper is 2.55 Å.[27] Using these in Eq. (11), one finds that $\alpha=0.20$. This agreement is as good as can be expected.

V. EXPERIMENTAL RESULTS

Total Thermal Conductivity

Table I lists the sample history. The letter in

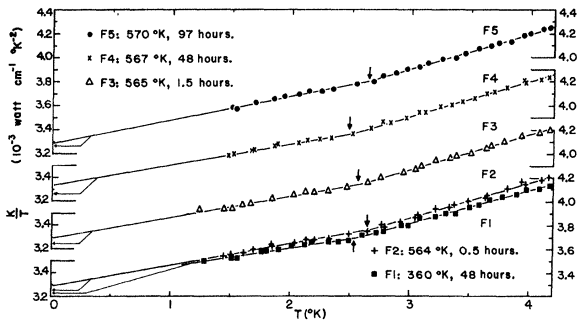

FIG. 6. Ratio of experimental total thermal conductivity K to absolute temperature T is plotted against T for specimens $F1-F5$. Horizontal arrows indicate the ratio L_0/ρ_0, where L_0 and ρ_0 are the ideal Lorenz number and the residual resistivity, respectively. Solid straight lines through the data were fit by the method of least squares. There is a change in slope at the temperature indicated by the small vertical arrows. Annealing temperature and time in oven are indicated on the graph.

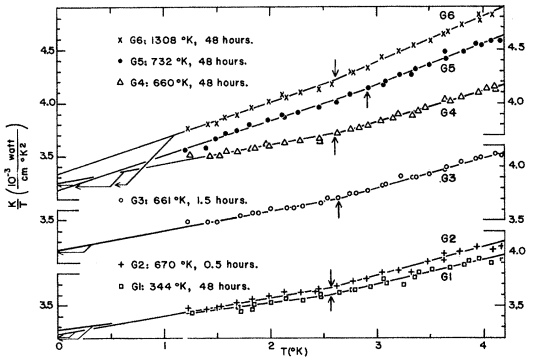

FIG. 7. Ratio of experimental total thermal conductivity K to absolute temperature T is plotted against T for specimens $G1$–$G6$. Horizontal arrows indicate the ratio L_0/ρ_0, where L_0 and ρ_0 are the ideal Lorenz number and the residual resistivity, respectively. Solid straight lines through the data were fit by the method of least squares. There is a change in slope at the temperature indicated by the small vertical arrows. Annealing temperature and time in oven are indicated on the graph.

each sample designation identifies the specimen (there were eight) and the number identifies the state of deformation or recovery of the specimen. The C and E series were a study of the variation of recovery of the conductivity with annealing temperature, and the F and G series were a study of recovery with time. Sample H is the single-crystal nickel specimen, used for control.

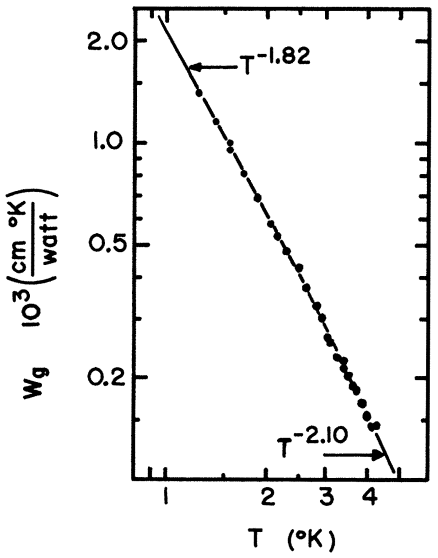

FIG. 8. Lattice thermal resistivity W_g (equal to $1/K_g$, where K_g is the lattice thermal conductivity) of sample D, a well-annealed specimen whose lattice conductivity is limited only by scattering of phonons by electrons, plotted against absolute temperature T. This is a log-log plot. There is a change in the temperature dependence of W_g at about $T = 2.6$ °K, the temperature of the change in slope of K/T (Fig. 4). This effect is thought to be associated with small electron mean free path in copper plus 10 at.% aluminum.

TABLE II. Thermal conductivity constants – results of the least-squares fits.

Sample number	$L_0{}^a/\rho_0$	$A_<{}^a$	$B_<{}^b$	$A_>{}^a$	$B_>{}^b$	T_K (K)
A	3.073	3.090[c]	0.035[c]	...	...	...
B	3.277	3.455	0.325	3.221	0.416	2.58
$C1$	3.272	3.445	0.013	3.165	0.225	2.29
$C2$	3.281	3.507	0.094	3.120	0.249	2.49
$C3$	3.276	3.371	0.201	3.011	0.333	2.72
$C4$	3.302	3.413	0.217	3.412	0.320	2.62
D	3.327	3.562	0.343	3.228	0.432	2.63
$E1$	3.223	3.256	0.147	2.994	0.247	2.62
$E2$	3.271	3.368	0.142	3.103	0.250	2.47
$E3$	3.261	3.323	0.168	3.044	0.267	2.58
$E4$	3.242	3.270	0.200	2.980	0.308	2.68
$E5$	3.279	3.395	0.337	3.202	0.414	2.50
$E6$	3.281	3.389	0.343	3.200	0.420	2.47
$E7$	3.286	3.420	0.344	3.221	0.419	2.63
$F1$	3.231	3.292	0.160	3.017	0.268	2.54
$F2$	3.244	3.286	0.180	2.989	0.292	2.65
$F3$	3.244	3.298	0.174	3.001	0.290	2.57
$F4$	3.261	3.337	0.171	3.041	0.291	2.49
$F5$	3.261	3.291	0.194	3.038	0.290	2.65
$G1$	3.199	3.266	0.133	3.005	0.235	2.57
$G2$	3.207	3.242	0.169	2.998	0.264	2.57
$G3$	3.212	3.229	0.179	2.968	0.278	2.64
$G4$	3.217	3.262	0.170	2.960	0.286	2.61
$G5$	3.237	3.187	0.322	3.017	0.381	2.91
$G6$	3.227	3.342	0.333	3.091	0.430	2.61
H	44.91	...	...	...	...	...

[a]Units of 10^{-3} W cm^{-1} °K^{-2}.
[b]Units of 10^{-3} W cm^{-1} °K^{-3}.
[c]There was no kink in the data of sample A, and thus these constants are to be used from 1 to 4 °K.

In Figs. 3–7 K/T is plotted against T, where K is the total thermal conductivity, and T is the absolute temperature. The horizontal arrows show the ratio L_0/ρ_0, which is K_e/T [see Eq. (2)]. The residual electrical resistivity ρ_0 was taken to be the measured total resistivity at 4.2 °K and is listed in Table I. Electrical resistivity was also measured at 1.1 °K, and a slight increase of less than 0.15% was noted in most cases. This was attributed to a small amount of iron which was added in the swaging. The data were linear, but there was change in slope for all specimens except A at a temperature T_K (listed in Table II) indicated by the small vertical arrows. Thus a least-squares fit to the data was made in two line segments

$$\frac{K}{T} = \begin{cases} A_> + B_> T & T > T_K \\ A_< + B_< T & T < T_K \end{cases}$$

The constants $A_>$, $B_>$, $A_<$, and $B_<$ for each sample are listed in Table II. This "kink" in the K/T vs

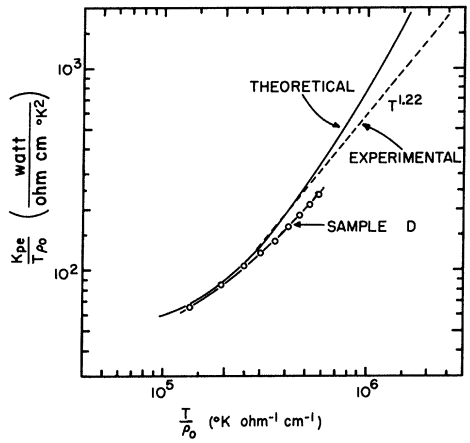

FIG. 9. Quantities K_{pe}, T, and ρ_0 are the lattice conductivity limited only by scattering of phonons by electrons, absolute temperature, and residual resistivity, respectively. Solid and dashed curves are the theoretical and empirical curves of Lindenfeld and Pennebaker (Ref. 23). Solid curve connecting open circles is the experimental lattice conductivity data of sample D, the well-annealed specimen in which dislocation scattering was negligible. This has a curvature which is qualitatively the same as that of the theory.

T data is thought to be an effect in the lattice thermal conductivity K_g because there was no variation of the electrical resistivity in the temperature

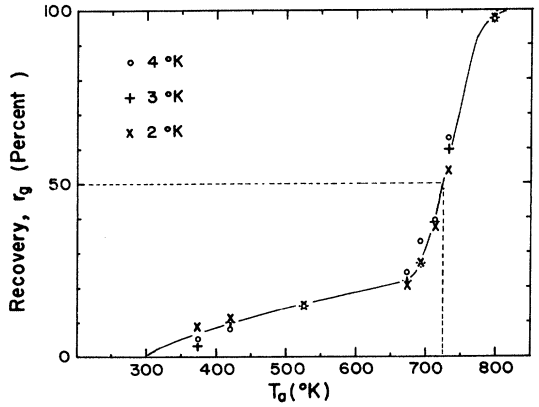

FIG. 10. Recovery r_g of lattice thermal conductivity of 9–10% plastically deformed specimens, plotted against annealing temperature T_a. Recovery is measured with respect to the state of the deformed specimens at 300 °K. All annealing times are longer than 12 h (essentially infinite annealing time). Points (○), (+), and (×) refer to the three different lattice conductivity measuring temperatures 4, 3, and 2 °K, respectively. Up to 700 °K the recovery is small; in this region it is thought that the rise of lattice conductivity is due to the rearrangement of impurities, not decrease of dislocation density. Between 700 and 800 °K the lattice conductivity recovers completely as a result of recrystallization. The recrystallization temperature is 725 °K.

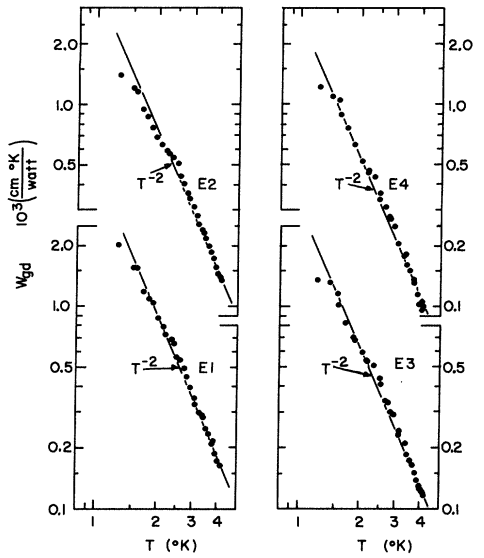

FIG. 11. Log-log plot of the dislocation lattice thermal resistivity W_{gd} against the absolute temperature T for specimens $E1$–$E4$. The temperature dependence of W_{gd} is very close to T^{-2}, as theory predicts. Specimen $E1$ was plastically deformed 9% at 77 °K and annealed at 300 °K for 12 h. Samples $E2$, $E3$, and $E4$ were annealed at 422, 552, and 673 °K, respectively, for 48 h at each temperature. The dislocation thermal resistivity is slightly greater than the phonon-electron thermal resistivity (Fig. 8). The solid lines are constrained to a T^{-2} temperature dependence.

range 1–4 °K which could produce such a large variation in the electronic conductivity [see Eq. (2)]. The kink will be discussed in more detail below.

Lattice Thermal Conductivity

The lattice thermal conductivity K_g was found from Eq. (3). In these specimens in this temperature range only electrons and dislocations scatter phonons significantly. Thus, Eq. (4) becomes

$$1/K_g \equiv W_g = W_{pe} + W_{gd} \quad . \tag{20}$$

In the well-annealed specimens B, D, $E5$, $E6$, $E7$, and $G6$ the dislocation density was low and W_{gd} was negligible. These specimens all had lattice thermal conductivities which were within 3% of each other, and a kink in a plot of K_g/T vs T. In a specimen which was plastically deformed about 9%, W_{gd} was slightly more than one-half of W_g. Sample D was taken to be the standard well-annealed specimen, and since $W_{gd} \ll W_{pe}$ in this case, we have

$$W_{pe} \approx (W_g)_D = (1/K_g)_D \quad , \tag{21}$$

where the D subscript refers to sample D. This thermal resistivity was not simply proportional to T^{-2} as predicted by Eq. (6). This is shown in Fig.

8. There is a change in the temperature dependence of W_{pe} at about 2.6 °K. In Fig. 9 the lattice thermal conductivity of specimen D is compared to the theory of Lindenfeld and Pennebaker.[23] Although quantitative agreement is not exact, specimen D has the same general curvature at about the same place as the theoretical and empirical curve. Thus, it is thought that the kink which was so evident in the K/T vs T graphs was an effect in the phonon-electron lattice thermal resistivity. There is another piece of information which supports this conclusion: Sample A was heavily cold worked, having been swaged from a 1 in. to a $\frac{1}{8}$ in. diam without annealing. Its K/T vs T graph had no kink (Fig. 3), and

$$K/T \approx L_0/\rho_0 + BT \ .$$

In this case we have $W_{pe} \ll W_{gd} \propto T^{-2}$.

Recovery of K_g

The recovery of K_g with annealing temperature (all annealing times were greater than 12 h, essentially infinite time) is shown in Fig. 10. The recovery is

$$r_g = \frac{(K_g)_Y - (K_g)_X}{(K_g)_D - (K_g)_X} \ ,$$

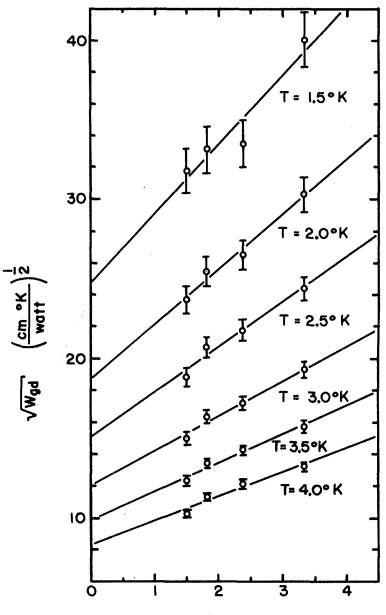

FIG. 12. Quantities W_{gd} and T_a are dislocation lattice thermal resistivity and the annealing temperature, respectively. The four data points at each of the six measuring temperatures are for samples $E1-E4$. Error bars are indicated. According to the theory of Ackerman and Klemens (Ref. 5), a plot of W_{gd} against $1/T_a$ is linear. The data do have such a linear variation. Solid lines are least-squares fits to the data.

where X, Y, and D refer to deformed-, partially annealed- and fully annealed- (sample D) state lattice conductivities. At 300 °K we have $r_g = 0$. There is a slow recovery up to 700 °K which is caused by a variation of the impurity distribution around a dislocation, and then between 700 and 800 °K there is a rapid recovery of the lattice conductivity to the fully annealed state. Above 800 °K there is less than 2% variation. The recrystallization temperature, defined as that annealing temperature at which recovery was 50% complete, is 725 °K. A metallographic study of the alloy supported these conclusions. The plastically deformed specimens had large fractured grains (0.08 mm) which did not change in physical appearance after more than 48 h of anneal at 300 and 673 °K, but which changed into smaller more perfect grains (0.04 mm) after anneal at 773 °K.

Lattice Dislocation Thermal Resistivity

The lattice dislocation thermal resistivity W_{gd} was obtained by combining Eqs. (20) and (21):

$$(W_{gd})_Y = \left(\frac{1}{K_g}\right)_Y - \left(\frac{1}{K_g}\right)_D \ ,$$

where Y refers to one of the deformed specimens which has attained equilibrium at temperature T_a. The resistivity W_{gd} found in this way is plotted in Fig. 11. Its temperature dependence is very close to T^{-2}.

Equation (14) can be rewritten as

$$(W_{gd})^{1/2} = I + M/T_a \ , \tag{22}$$

$$I \equiv (CN_d)^{1/2}\gamma/T \ , \tag{23}$$

$$M \equiv (CN_d)^{1/2}(1/T)(\gamma\alpha^2 - \alpha\beta)c_0 v_0 B/k_B \ , \tag{24}$$

$$M/I = (1/\gamma)(\gamma\alpha^2 - \alpha\beta)c_0 v_0 B/k_B \ . \tag{25}$$

If the theoretical prediction Eq. (22) is consistent with the experimental data, a plot of $(W_{gd})^{1/2}$ vs $1/T_a$ should be linear. In Fig. 12 it can be seen that this is approximately true. The ratio of the slope M to the intercept I is quite constant, as it should be according to Eq. (25). Its average value is $(M/I)_{av} \approx 183 \pm 5$ °K (the error is the standard deviation). As in Sec. IV, Eq. (25) is a quadratic equation in α and its positive solution is $\alpha = 0.23$ (the negative solution is -0.07). Thus the present dependence on annealing temperature is in good agreement with the values of α found from the data of Charsley *et al.* which showed the variation of dislocation resistivity with concentration ($\alpha = 0.24$) and the x-ray data ($\alpha = 0.20$), as discussed in Sec. IV.

According to Eqs. (23) and (24), the slope and intercept should be proportional to T^{-1}. Figure 13 shows that the data do have this temperature dependence. Furthermore, from Eq. (14) the dislocation density can be estimated to be $N_d \approx 6 \times 10^{10}$ cm^{-2}.

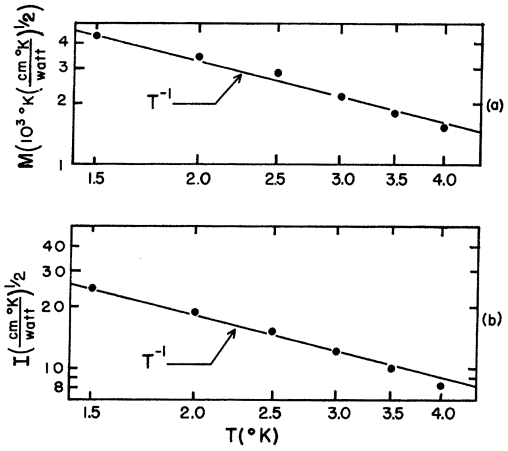

FIG. 13. Data points (a) $\log_{10}(M)$, and (b) $\log_{10}(I)$, plotted against $\log_{10}(T)$, where M is the slope and I is the intercept of lines drawn through the W_{gd} vs $1/T_a$ data, T is the measuring temperature, and T_a is the annealing temperature. According to the Ackerman and Klemens theory (Ref. 5), M and I should have a T^{-1} temperature dependence. The solid lines are constrained to have a T^{-1} temperature dependence; the data all lie close to these lines.

In Fig. 14 the recovery

$$f_g = \frac{(K_g)_Y - (K_g)_X}{(K_g)_Z - (K_g)_X}$$

is plotted against the annealing time; the subscripts X, Y, and Z refer to the states at zero, intermediate, and infinite anneal times at a fixed anneal temperature. Figure 14 shows the isothermal recovery with anneal time for two temperatures: (a) 565 °K, and (b) 665 °K. It can be seen that the recovery is more than 65% complete after the first half-hour of anneal. However, the experimental error is large. In (a) the error bars cover the entire ordinate, and in part (b) the error is indicated.

In order to compare the data to the time-dependent theory, Eq. (16) was rewritten in the form

$$F\,(W_{gd}/W_{gd\infty})^{1/2} = e^{-t_a/\tau_0} ,$$

where

$$W_{gd} = CN_d(\gamma+\gamma')^2/T^2 ,$$

$$F \equiv \frac{T_{a1}}{T_{a2}-T_{a1}}\left\{\frac{T_{a2}}{183}\left[\left(1+\frac{183}{T_{a2}}\right)\left(\frac{W_{gd}}{W_{gd\infty}}\right)^{1/2}-1\right]-1\right\} .$$

If the theory is consistent with the data, a plot of ln F against t_a, the anneal time, should be a straight line through the origin. In Fig. 15 it can be seen that the data are not linear, neither (a) for $T_{a2}=565$ °K nor (b) for $T_{a2}=665$ °K. Furthermore, the T^2 measuring temperature dependence of $1/\tau_0$ (the slope) is not obeyed [see Eq. (17)]. In the case of the 565 °K anneal, the dependence of τ_0 on T is even reversed. The failure of the theory may be a result of the assumption of a unique diffusion constant; since deformation produces excess vacancies, the diffusivity may depend on the history of the specimen. However, considering the large experimental error it is difficult to draw any firm conclusions.

VI. SUMMARY

The lattice conductivity of copper plus 10 at.% aluminum which had been plastically deformed 9% in tension after anneal at 930 °C for 48 h was found to recover slowly between 300 and 700 °K (48 h at each temperature), and then rapidly return to its fully annealed value between 700 and 800 °K. The rapid variation was caused by recrystallization, and the recrystallization temperature was found to be 725 °K.

A change in slope of a line through the K_g/T vs T data of well-annealed and 9–10% plastically deformed specimens was found. This was thought to arise from an effect in the phonon-electron lattice thermal resistivity which was associated with the smallness of the electron mean free path relative to the phonon wavelength in this impure alloy [see the discussion of Eq. (7)]. The theory of Lindenfeld and Pennebaker,[23] which employed the Pippard formula[22] for phonon mean free path for scattering of phonons by electrons, explained the kink qualitatively if not quantitatively. In the realm of short

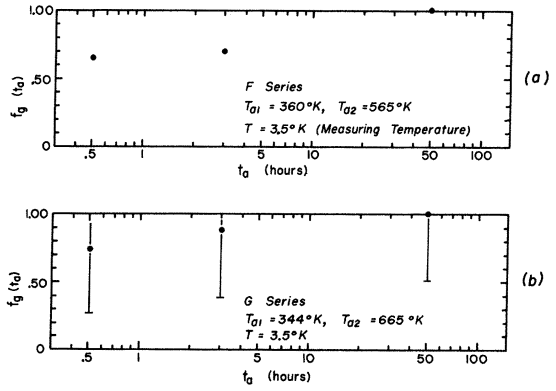

FIG. 14. Quantity f_g plotted against $\log_{10}(t_a)$, where f_g is defined as

$$f_g = [(K_g)_Y - (K_g)_X]/[(K_g)_Z - (K_g)_X];$$

t_a is the annealing time and subscripts X, Y, and Z refer to the state of zero anneal time at annealing temperature T_{a2} (infinite anneal time at T_{a1}), the state of finite anneal time at T_{a2}, and the state of infinite anneal time at T_{a2} (longer than 12 h), respectively. In (a) we have $T_{a1}=360$ °K and $T_{a2}=565$ °K; the error bars cover the entire ordinate. In (b) we have $T_{a2}=665$ °K; error bars are indicated. The measuring temperature T is 3.5 °K in both cases.

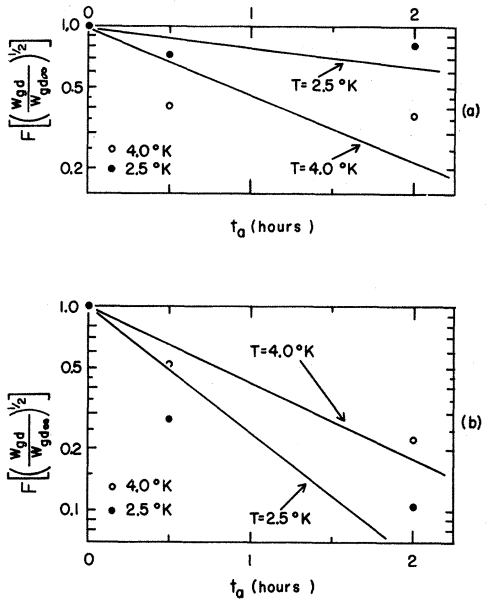

FIG. 15. If Klemens's theory (Ref. 4) is consistent with the experimental data, a plot of $\log_{10}(F)$ (F is defined in the text) against the annealing time t_a would be a straight line passing through the point $\log_{10}(F)=0$, $t_a=0$. The data do not lie on a straight line through the origin. The slope of the lines drawn through the data and constrained to pass through the origin is $1/\tau_0$, where τ_0 is the annealing relaxation time. Theoretically, $1/\tau_0$ is proportional to T^2. In case (a) we have $T_{a1}=160$°K and $T_{a2}=565$ °K, the annealing temperatures at $t_a=0$ and $t_a>0$, respectively; $1/\tau_0$ is roughly proportional to T^2 between 2.5 and 4 °K, but not between 1.5 and 2.5 °K (the 1.5 °K point is not shown). In case (b) we have $T_{a1}=344$ °K and $T_{a2}=665$ °K; $1/\tau_0$ is not proportional to T^2 between 2.5 and 4 °K. However, the experimental error (see Fig. 14) is so large that no definite conclusions can be drawn.

electron mean free paths the usual theory for phonon-electron lattice thermal resistivity, which predicts a T^{-2} temperature dependence, is thought not to hold.

The small recovery of K_g between 300 and 700 °K (see Fig. 10) was explained by a redistribution of impurities around a dislocation which resulted in a decrease of phonon scattering. The variation of the dislocation lattice thermal resistivity with annealing temperature was well explained by recent theories of Klemens,[3] and Ackerman and Klemens.[5] It was possible to estimate the fractional atomic size difference α between the aluminum and copper to be $\alpha=0.23$. Using the same theory and the experimental work of Charsley *et al.*[2] on the concentration dependence of dislocation lattice thermal resistivity per dislocation, it was possible to estimate that $\alpha=0.24$. The experimental x-ray data on the change of lattice spacing with the addition of the aluminum to copper yielded $\alpha=0.20$. These independent measurements are in good agreement.

The recent theory of Klemens[4] for the variation of the dislocation lattice thermal resistivity with annealing time at fixed annealing temperature was not consistent with the data; however, the experimental error was large.

Thus, although the kinetics of the impurity redistribution around the edge dislocation is not understood, something can be said about the spatial distribution. Around an edge dislocation there are regions of compression and expansion of the lattice. The aluminum atoms, which are larger than the copper atoms, will fit more easily into the expanded regions, and since the elastic strain decreases as the distance from the dislocation core increases, the deviation of the impurity concentration from its homogeneous value will be greatest in the region of the core. As the annealing temperature is increased, the impurities diffuse around the dislocation from the expanded to the compressed regions and the dislocation scattering decreases.

ACKNOWLEDGMENTS

The authors gratefully acknowledge the technical assistance of H. Taylor, J. D'Anna, P. Smith, M. Simard, D. Strom, K. Johnson, A. Lohanick, A. Friedman, B. Brown, and Miss L. Harrington. The Metallurgy Department of the University of Connecticut generously made their facilities available to us, and in particular L. McCurdy and W. Ovens were very helpful. The computer work in this study was all done using the facilities of the University of Connecticut Computer Center under NSF Grant No. GJ-9.

---

*Research supported by AFOSR, USAF under Contract No. F 44620-69-C-0011 and by ONR under Contract No. NONR 2967(00). Work is part of a thesis which was submitted by M. A. Mitchell in partial fulfillment of the requirements for the Ph. D. at the University of Connecticut.

†Present address: Naval Ordnance Laboratory, White Oak, Silver Spring, Md.

[1]P. G. Klemens, in *Solid State Physics*, edited by F. Seitz and D. Turnbull (Academic, New York, 1958).

[2]P. Charsley, J. A. M. Salter, and A. D. W. Leaver, Phys. Status Solidi 25, 531 (1968).

[3]P. G. Klemens, J. Appl. Phys. 39, 5304 (1968).

[4]P. G. Klemens, J. Appl. Phys. 40, 4696 (1969).

[5]M. Ackerman and P. G. Klemens, J. Appl. Phys. (to be published).

[6]J. M. Ziman, *Electrons and Phonons* (Clarendon, Oxford, England, 1960).

[7]P. G. Klemens, in *Handbuch der Physik*, edited by S. Flügge (Springer, Berlin, 1956), Vol. XIV.

[8]A. H. Cottrell, *Dislocations and Plastic Flow in Crystals* (Clarendon, Oxford, England, 1953).

[9]W. G. R. Kemp, P. G. Klemens, R. J. Tainsh, and G. K. White, Acta Met. 5, 303 (1957).
[10]J. N. Lomer and H. M. Rosenberg, Phil. Mag. 4, 467 (1959).
[11]W. R. Kemp, P. G. Klemens, and R. J. Tainsh, Phil. Mag. 4, 845 (1959).
[12]L. M. Clarebrough, M. E. Hargreaves, and G. W. West, Phil. Mag. 1, 528 (1956).
[13]J. E. Gueths, N. N. Clark, D. Markowitz, F. V. Burckbuchler, and C. A. Reynolds, Phys. Rev. 163, 364 (1967).
[14]E. J. Walker, Rev. Sci. Instr. 30, 834 (1959).
[15]F. G. Brickwedde, H. van Dijk, M. Durieux, J. R. Clement, and J. K. Logan, J. Res. Natl. Bur. Std. (U.S.) 64A, (1960).
[16]P. G. Garbarino and C. A. Reynolds (unpublished).
[17]J. C. Erdman and J. A. Jahoda, in *Proceedings of the Seventh Conference on Thermal Conductivity*, NBS Special Pub. No. 302 (U. S. GPO, Washington, D. C., 1968), p. 259.
[18]H. Margenau and G. M. Murphy, *The Mathematics of Physics and Chemistry* (Van Nostrand, Princeton, N.J., 1956).
[19]J. E. Gueths, C. A. Reynolds, and M. A. Mitchell, Phys. Rev. 150, 346 (1966).
[20]R. E. B. Makinson, Proc. Cambridge Phil. Soc. 34, 474 (1938).
[21]P. G. Klemens, Australian J. Phys. 7, 57 (1954).
[22]A. B. Pippard, Phil. Mag. 46, 1104 (1955).
[23]P. Lindenfeld and W. B. Pennebaker, Phys. Rev. 127, 1881 (1962).
[24]P. G. Klemens, Proc. Phys. Soc. (London) A68, 1113 (1955).
[25]Two different models were used for the interaction Hamiltonian in Refs. 24 and 1. The latter, which is better founded theoretically, gives values of C larger by a factor of 16, but this difference is only stated in the text: The formulas given in Ref. 1 are those of Ref. 24, resulting in considerable confusion.
[26]H. M. Rosenberg, *Low Temperature Solid State Physics* (Clarendon, Oxford, England, 1963).
[27]W. B. Pearson, *A Handbook of Lattice Spacings and Structures of Metals and Alloys* (Pergamon, New York, 1958), Vol. 4.

PHYSICAL REVIEW B VOLUME 3, NUMBER 4 15 FEBRUARY 1971

Theoretical Strength of a Perfect Crystal *

Frederick Milstein
University of California, Santa Barbara, California 93106
(Received 3 August 1970)

A mathematical procedure is presented for applying the Born stability criteria to the determination of the mechanical stability of cubic crystals in the presence of applied forces and deformations. The general procedure presented is suitable for use in conjunction with an electronic computer and is independent of the specific model of interatomic interactions which may be used in numerical calculations. In the present study, specific calculations are performed for a body-centered-cubic (bcc) crystal lattice with an uniaxial force applied perpendicular to a face of a unit cell. The atoms in the crystal are assumed to interact via the two-body Morse interatomic-potential function determined by Girifalco and Weizer [Phys. Rev. 114, 687 (1959)] for bcc iron. Two ranges of stability, a bcc phase and a body-centered-tetragonal (bct) phase, were found to exist. The bct phase has a theoretical strength of 0.9×10^{11} dyn/cm^2 with a corresponding theoretical strain of about 7%. These values are fairly close to the values of 1.3×10^{11} dyn/cm^2 tensile strength and about 5% strain experimentally observed for iron whiskers.

I. INTRODUCTION

Necessary conditions for the thermodynamic stability of a crystal lattice are that the crystal be mechanically stable with respect to arbitrary (small) homogeneous deformations. These conditions are often referred to as the "Born stability criteria" after Born[1] who derived mathematical expressions for these stability requirements for cubic lattices of the Bravais type on the assumption of central forces of a very general type. Misra[2] applied the Born stability criteria to the study of mechanical stability of cubic crystals with inverse-power-law interactions between atoms, and more recently the present author[3] used these criteria to study the stability of cubic crystals with Morse-potential interatomic interactions. These studies were for unstressed (and hence undeformed) crystal lattices.

The present paper is concerned with applying the Born stability criteria to the study of mechanical stability of cubic crystals which are deformed homogeneously under the application of external forces. This study is of interest because the values of stress and strain at which the crystal becomes mechanically unstable, in terms of the Born criteria, represent the "theoretical strength" of the crystal.[4] The failure of a real material under the